Thermodynamic properties of hydrogen in quasi-two-dimensional vanadium lattices

1995 J. Phys.: Condens. Matter 7 8139

(http://iopscience.iop.org/0953-8984/7/42/010)

J. Phys.: Condens. Matter 7 (1995) 8139–8150. Printed in the UK

Thermodynamic properties of hydrogen in quasi-two-dimensional vanadium lattices

F Stillesjö, S Ólafsson, P Isberg and B Hjörvarsson
Department of Physics, Uppsala University, Box 530, S-751 21 Uppsala, Sweden

Received 26 June 1995

Abstract. The solubility and thermodynamics of hydrogen in quasi-two-dimensional vanadium lattices have been investigated. The quasi-two-dimensional character of the vanadium lattices were obtained by growing alternating layers of molybdenum and vanadium in Mo/V superlattice structures. The hydrogen solubility was found to be higher in the thin V layers than in bulk vanadium. The enthalpy change, $\Delta\bar{H}_H$, reached a value of -0.42 eV per H atom after a steep increase from the infinite-dilution limit (-0.28 eV per H atom). The entropy change, $\Delta\bar{S}_H$, is found to decrease for the thin V layers compared to bulk vanadium for hydrogen concentrations up to H/V = 0.2. Above 0.2, $\Delta\bar{S}_H$ reached the bulk values.

1. Introduction

Hydrogen in vanadium can be studied under novel conditions in epitaxially grown Mo/V single-crystal superlattices. Previous investigations of hydrogen in Mo/V superlattices show that hydrogen is localized in the vanadium layers [1, 2]. This is due to the endothermic heat of solution for hydrogen in molybdenum (+0.48 eV per H atom) [3]. As the hydrogen is exclusively found in the vanadium layers, the resulting modulation of the hydrogen concentration perpendicular to the substrate plane in the superlattice is of a one-dimensional character. The vanadium layers in a Mo/V superlattice constitute therefore a quasi-two-dimensional metal host for the hydrogen atoms, isolated from each other by spacer layers of molybdenum. This is illustrated in figure 1. The Mo/V superlattice system is therefore well suited as a model system for studies of the influence of boundary conditions on the phase transitions and the hydrogen–hydrogen (H–H) interaction in a metal–hydrogen system. The implications of strong boundaries on the H–H interaction have previously been treated theoretically by Alefeld [4], but experimental studies have not been realized until now.

In previous investigations of hydrogen in Mo/V superlattices, we have focused on charge transfer effects on the hydrogen solubility next to the interfaces [1–3, 5]. We found that there is a region in the vanadium layers that does not contain hydrogen. Furthermore, the hydrogen-induced lattice expansion of vanadium in the superlattices was found to be small for hydrogen concentrations H/V > 0.5 compared to bulk [1].

The results presented here are the first thermodynamic characterization of hydrogen in a metal host of two-dimensional character. Resistometric techniques were used to measure the hydrogen solubility isotherms of Mo/V superlattices with vanadium layer thicknesses of five unit cells (u.c.) and seven u.c. to include the layer thickness dependence on the hydrogen solubility. The hydrogen solubility was found to be significantly higher in both of the Mo/V superlattices compared to the solubility of hydrogen in bulk vanadium. The enthalpy change, $\Delta\bar{H}_H$, and entropy change, $\Delta\bar{S}_H$, as a function of hydrogen concentration

0953-8984/95/428139+12$19.50

were determined from the solubility isotherms. The change in enthalpy $\Delta\bar{H}_H$ in vanadium in the superlattice was larger than in the bulk vanadium change, while the change in entropy $\Delta\bar{S}_H$ was lower than the corresponding bulk entropy.

The remainder of this paper is organized as follows. In section 2, the theoretical background of the resistivity of interstitial alloys will be outlined. In section 3, all the experimental details are emphasized and in section 4 we present the experimental results. In section 5, we discuss the results and finally, in section 6, we give a summary and conclusion.

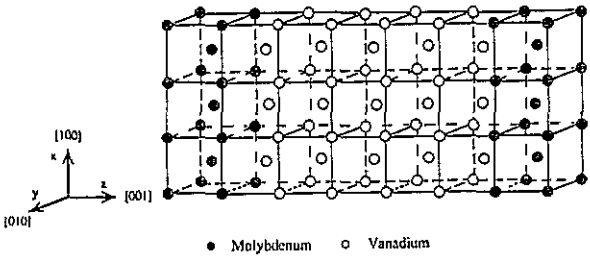

Figure 1. A quasi-two-dimensional vanadium layer in a Mo/V superlattice. The vanadium layer thicknesses studied are 1.5 nm and 2.1 nm respectively, which corresponds to five and seven unit cells of vanadium. The hydrogen is localized in the vanadium layer and with a reduced hydrogen content next to the Mo interface. For details, see text.

2. Theoretical background

The scattering probability for the electrons in a metal changes when impurity atoms replace the host atoms substitutionally. This experimental observation can be described with the empirical expression

$$\rho_{tot} = \rho_i + \rho_L(T) \tag{1}$$

which is known as Matthiesen's law. Here, ρ_i (where the subscript i stands for impurity) contains all temperature-independent contributions to the resistivity present in the lattice, such as vacancies and impurity atoms, and $\rho_L(T)$ (where T denotes the temperature) is the temperature-dependent part of the resistivity, originating from the electron–phonon scattering. For a moderately low concentration of defects in a crystal, $\rho_L(T)$ is independent of the defect or impurity concentration. For a disordered substitional alloy, the impurity part, ρ_i, of the resistivity can be written as [6]:

$$\rho_i = \Delta\rho \sim \text{constant} \times (N_A + N_B)x(1-x). \tag{2}$$

Here, N_A and N_B is the number of A and B atoms, and x and $(1-x)$ the mole fractions of the constituents (A and B respectively). The impurity part of the resistivity is called the *excess resistivity*, $\Delta\rho$. This expression is in qualitative agreement with experimental data and also in some cases in quantitative agreement [7]. For interstitial alloys, the interstitial atoms are assumed to act as randomly distributed scattering centres at small concentrations. The excess resistivity is therefore proportional to the impurity concentration. For a metal–hydrogen (M–H) system, where the number of hydrogen atoms can be as high as the number of metal

atoms, a linear relationship between the excess resistivity and the hydrogen concentration cannot be expected. Pryde and Tsong [8] have developed a model for high concentration interstitial alloys based on (2), and applied it to M–H systems. They argued that the mole fraction of A and B atoms in the substitutional alloy can be replaced by the filled and empty interstitial sites of hydrogen in the M–H system. These sites then correspond to the components of a binary alloy. Proceeding in the same way as for substitutional alloys with this modification inserted, the excess resistivity is then

$$\Delta\rho = Kc(n - c) \tag{3}$$

where K is a constant that depends on the difference in crystal potential between empty and filled sites of hydrogen. The hydrogen concentration is $c = N_H/N_M$, where N_H is the number of filled hydrogen sites in the lattice and N_M the number of metal atoms. The hydrogen concentration is related to the fractional occupancy of sites, θ ($\theta = N_H/N_s$ where N_s is the total number of interstitial sites), by $c = n\theta$ where n is the number of hydrogen atoms per metal atom in the crystal.

The maximum excess resistivity is obtained for an average occupancy $\theta = 0.5$ of the interstitial sites. Above 0.5, the excess resistivity decreases. The electrons scatter now mainly on the vacant interstitial sites. At the maximum occupancy, $\theta = 1$, the excess resistivity should vanish. However, the excess resistivity does not necessarily need to vanish at the maximum filling $\theta = 1$, since changes in the electronic structure at high fillings affect the temperature-dependent part of the resistivity as well as the constant K in (3).

This model has successively been applied to the analysis of excess resistivity dependence on hydrogen concentration in the tantalum–hydrogen system [8]. More recently, the model was also applied to interpret resistivity measurements on Ta–H thin films [9].

The resistivity of thin metallic layers is generally larger than the bulk values. For a multilayered system, the resistivity is highly dependent on the thicknesses of the individual layers. If the mean free path of the electrons is larger than the individual layer thickness, the electrons can freely move within the layer but will suffer some scattering at the interfaces. The presence of interfaces increases the resistivity and this increase is strongly dependent on the coherency of the interfaces. Resistivity measurements on multilayers with modulation wavelengths Λ of roughly 10 nm down to 3 nm are characterized by a $\rho \sim 1/\Lambda$ dependence [10]. The interface scattering can therefore be assumed to be a temperature-independent contribution to the total resistivity of the multilayer. The introduction of hydrogen in a multilayer further increases the resistivity of the system. This increase of the resistivity is exclusively associated with hydrogen as impurity atoms given that no major change in the electronic structure occurs. In this work, we use a modified version of the model for interstitial alloys developed by Pryde and Tsong to deduce the hydrogen concentration in the Mo/V superlattices. The relation between the excess resistivity and the hydrogen content was determined by measuring both the resistivity and the hydrogen concentration independently, as will be described in the next section.

3. Experimental details

Symmetrical ($L_V/L_{Mo} = 1$) Mo/V superlattices were grown epitaxially on polished MgO(001) substrates with dual-target DC magnetron sputtering at an argon gas pressure of 5×10^{-3} mbar. Samples with modulation wavelengths $\Lambda(= L_V + L_{Mo})$ of 3.0 nm and

4.2 nm (1.5/1.5 and 2.1/2.1 nm of Mo and V respectively) were made, which corresponds to five and seven unit cells (u.c.) of each constituent. These samples will be referred to as 5 u.c. and 7 u.c. The substrate temperature was 700 °C and the deposition rate was 0.1–0.2 nm s^{-1} during growth. The samples were finally covered with a 10 nm V cap in order to get well defined surface conditions. The total thickness was 500 nm for each superlattice. After deposition, the quality of the superlattice structures was investigated using low- and high-angle x-ray diffraction. The measurements showed a good single-crystalline quality and a sharp chemical modulation similar to previous reported results [11]. The samples were finally cleaved to 10 mm × 2 mm stripes for the resistivity measurements.

All of the resistivity measurements were done in an all metal–ceramic ultra-high vacuum compatible gas system with possibilities for hydrogen loading. The gas system was pumped with a 631 s^{-1} turbopump, which gave a base pressure of 5×10^{-8} mbar after bakeout with a residual gas content consisting of 99.9% H_2. Hydrogen gas of 99.995% initial purity was used for all the measurements. Additional purification was obtained with a liquid nitrogen cooled molecular sieve (Supelco 30/40 mesh) trap. The samples were mounted on a ceramic holder with tungsten wire connectors in a four-point probe pressed against the film. The sample was heated in vacuum up to elevated temperatures with an external resistivity heated oven and the surface temperature of the sample was continuously measured with an internally mounted and uncompensated chromel–alumel thermocouple with an accuracy of ±1.5 °C. The voltage drop was registered using a Stanford Research System SR 830 DSP lock-in amplifier with a resolution of 0.1% of full scale. The applied current was 250 μA, which resulted in a typical voltage drop over the sensing contacts of 0.5 mV.

After mounting the sample onto the ceramic holder, the hydrogen cell was evacuated to 5×10^{-8} mbar and flushed several times at room temperature with purified H_2 gas. The sample was thereafter annealed at 500 °C for one hour and flushed several times with hydrogen purified through the molecular sieve trap to remove surface oxides and to activate the sample surface. Hydrogen gas was introduced after cooling the sample down to the actual temperature. The hydrogen pressure was measured using a CCM capacitive pressure gauge with a pressure span 0–1000 Torr. The accuracy of the pressure determination was 0.1% of reading. The time between the pressure steps was typically 5–10 min to reach equilibrium, but times as long as 50 min were needed at the lowest temperatures. Isotherms ranging from 350–500 °C in steps of 50 °C were measured. Both absorption and desorption isotherms were recorded.

The hydrogen concentration in the samples was measured using the $^1H(^{15}N, \alpha\gamma)^{12}C$-nuclear resonance reaction. The measurements were performed at characteristic points of the excess resistivity isotherms. By this procedure we related the change in resistivity to the hydrogen concentration in the samples. The details of the ^{15}N-method for hydrogen profiling are presented elsewhere [12].

4. Experimental results

A typical resistivity measurement for the 7 u.c. superlattice is presented in figure 2. The temperature was 325 °C during the measurement. The data are presented as the change in resistivity $\Delta\rho$ (or the excess resistivity discussed in section 2), against time. The hydrogen gas pressure is increased in discrete steps from zero to a maximum pressure of 1000 Torr. The resistivity increased when the hydrogen gas was introduced and levelled off when equilibrium was established. The excess resistivity increased up to a maximum value of 2.2 $\mu\Omega$ cm at a hydrogen gas pressure of 100 Torr. Thereafter, the resistivity change

decreased reaching a value of 0.5 $\mu\Omega$cm at 1000 Torr. Before equilibration, the resistivity signal changed exponentially with time. Typical uptake rate constants were 10 min at the lowest pressures. The uptake rate increased with increasing hydrogen gas pressure, reaching a value of 25 s at 100 Torr and above.

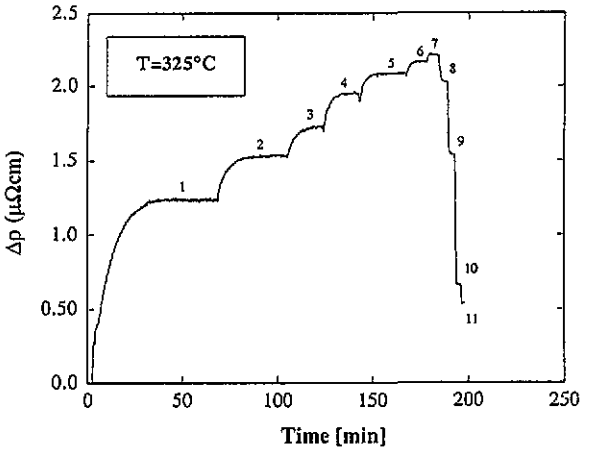

Figure 2. The excess resistivity as a function of time for the 7 u.c. superlattice sample. The hydrogen pressure is increased in steps to (1) 6 Torr, (2) 10 Torr, (3) 15 Torr, (4) 25 Torr, (5) 36 Torr (6) 50 Torr, (7) 100 Torr, (8) 200 Torr, (9) 400 Torr, (10) 905 Torr and (11) 1000 Torr.

The initial excess resistivity isotherms showed hysteresis effects of a few per cent, which diminished after 4–5 cycles. The measurements were randomly repeated several times to investigate the reproducibility. All isotherms agreed within a few per cent.

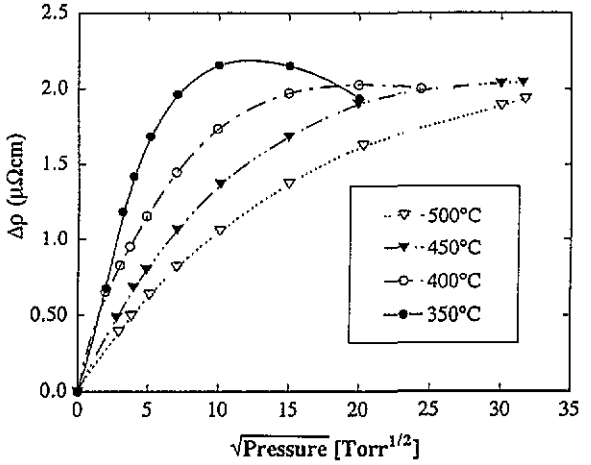

Figure 3. Excess resistivity isotherms as a function of the square root of the hydrogen pressure for the 7 u.c. Mo/V superlattice.

A selection of excess resistivity isotherms are presented in figure 3 for the 7 u.c. superlattice. The excess resistivity for the isotherms 400–500 °C increased monotonically

with increasing hydrogen pressure and levelled off around 2.0 $\mu\Omega$ cm. For the 350 °C isotherm, the excess resistivity reached a maximum value of 2.2 $\mu\Omega$ cm and decreased for higher pressures. The excess resistivity isotherms for the 5/5 u.c. superlattice are almost identical to the 7 u.c. data and are therefore not displayed here.

Measurements of the excess resistivity at lower temperatures show that the maximum excess resistivity increases with decreasing temperature and can be described by the following parametrized form in the temperature region 60 °C < T < 500 °C:

$$\Delta\rho_{max}(T) = 4.2 - 8.0 \times 10^{-1}T + 7.2 \times 10^{-6}T^2 \quad (\mu\Omega\,\mathrm{cm}) \tag{4}$$

where T is given in °C. To investigate this behaviour further, the samples were loaded with hydrogen to the maximum excess resistivity value at 350 °C and 280 °C for the two samples. Thereafter, the hydrogen concentration was determined using the $^1H(^{15}N, \alpha\gamma)^{12}C$ nuclear resonance reaction. The average hydrogen content in the vanadium layers of the superlattices were determined to $\langle H/V\rangle = 0.29$ at 350 °C and $\langle H/V\rangle = 0.34$ at 280 °C for the 5 u.c. sample, and $\langle H/V\rangle = 0.35$ at 350 °C and $\langle H/V\rangle = 0.37$ at 280 °C for the 7 u.c. sample.

Previous measurements of the hydrogen distribution in Mo/V multilayered superlattices show that there is a hydrogen-depleted region in vanadium in the vicinity of the molybdenum interface [1, 2]. The extent of this region is about 0.3 nm for the temperatures and pressures used here, and is considered to be constant independent of the vanadium layer thicknesses. The two outer layers were therefore considered to be devoid of hydrogen for both samples so that the results for the 5 u.c sample were scaled by a factor of 5/3 and those for the 7 u.c sample by a factor of 7/5. The average hydrogen content in the interior of the vanadium layers could therefore be determined to 0.48 (350 °C) and 0.57 (280 °C) for the 5 u.c. sample and 0.49 (350 °C) and 0.52 (280 °C) for the 7 u.c. sample. The hydrogen content in this interior region is the relevant parameter for the thermodynamic properties of the thin vanadium layers. We will exclusively refer to the hydrogen content in this region in the rest of this paper. Furthermore, the uncertainties in the determination of the $\langle H/V\rangle$ ratio from the excess resistivity are largest close to H/V = 0.5 since $\partial(\Delta\rho)/\partial c|_T$ is close to zero at this concentration. The hydrogen content at the excess resistivity maximum at 280 °C and 350 °C for the 5 and 7 u.c. samples are therefore, within the experimental uncertainties, the same.

We have therefore shown that the excess resistivity, $\Delta\rho$, is not independent of temperature at a fixed concentration as predicted by (3), but is rather given by:

$$\Delta\rho = 4\Delta\rho_{max}(T)c(n-c). \tag{5}$$

This is in contrast to previously published excess resistivity data for bulk and bulk-like materials [8, 9]. The hydrogen concentration was also measured for excess resistivities at several points below the maximum value. The results agreed well with (5), which was used to deduce the hydrogen content of the samples from the measured excess resistivity.

Hydrogen solubility isotherms were deduced from the resistivity data, and are presented in figure 4 for the 7 u.c. V layers and in figure 5 for the 5 u.c. V layers. The bulk isotherms from Veleckis and Edwards [13] are inserted for comparison purposes. The isotherms show that a larger amount of hydrogen can be solved in the superlattices than in bulk vanadium at the same pressure.

The enthalpy and entropy changes for the 5 u.c. and 7 u.c. vanadium lattices were deduced from the solubility isotherms using the van't Hoff relation:

$$\tfrac{1}{2}\ln p = \frac{\Delta\bar{H}_H}{k_B T} - \frac{\Delta\bar{S}_H}{k_B T}. \tag{6}$$

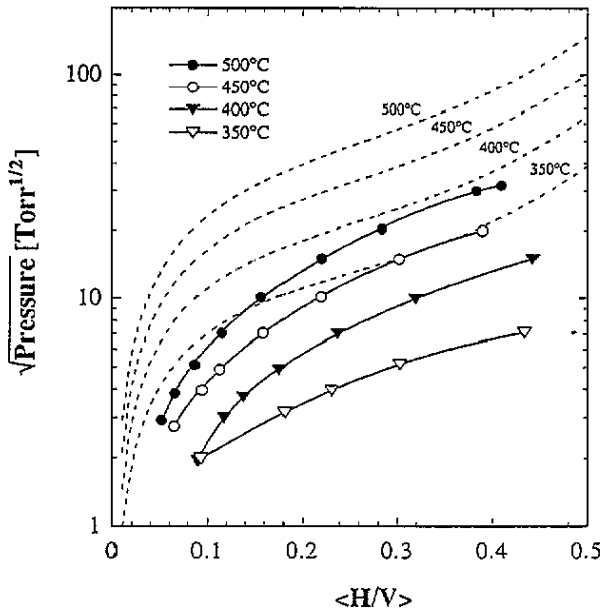

Figure 4. Hydrogen solubility isotherms for the 7 u.c. Mo/V superlattice deduced from the resistivity data. The broken curves are bulk vanadium hydrogen solubility isotherms taken from Veleckis and Edwards [5].

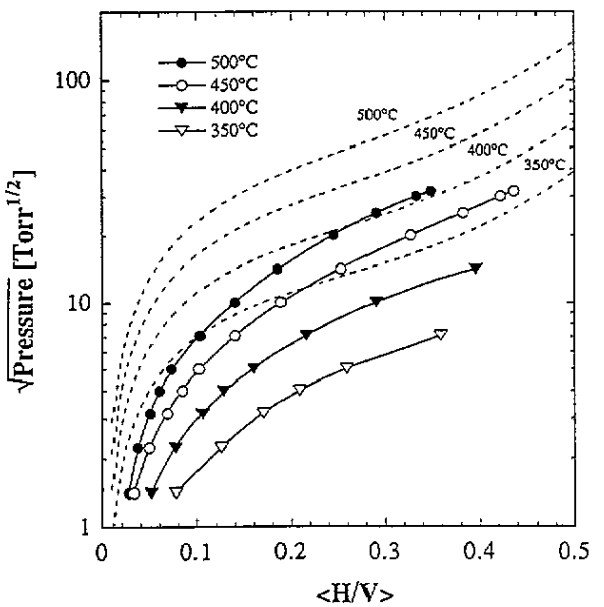

Figure 5. Hydrogen solubility isotherms for the 5 u.c. Mo/V superlattice together with the bulk vanadium isotherms. These results are deduced from the resistivity data.

Here, p is the pressure of the hydrogen gas, T the hydrogenation temperature, $\Delta\bar{H}_H$ the enthalpy change, $\Delta\bar{S}_H$ the entropy change and k_B the Boltzmann constant. Examples of

these analyses are presented in figure 6, the 5 u.c. sample. The full curves in the plot are linear fits of (6) to the data. Similar diagrams were calculated from the solubility isotherms of the 7 u.c. superlattice.

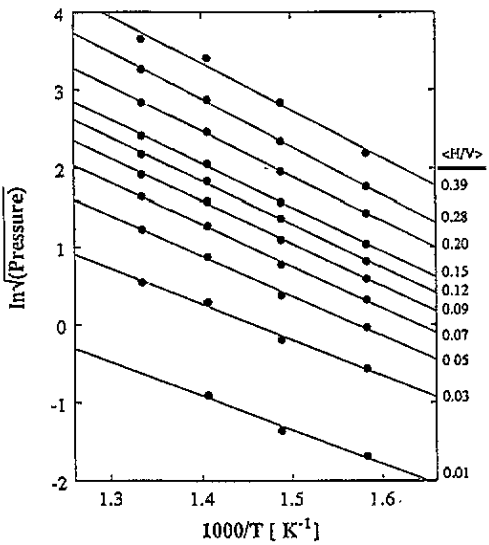

Figure 6. A van't de Hoff-plot for the 5 u.c. Mo/V superlattice showing the logarithm of the square root of hydrogen pressure as a function of the reciprocal temperature for different hydrogen concentrations ⟨H/V⟩.

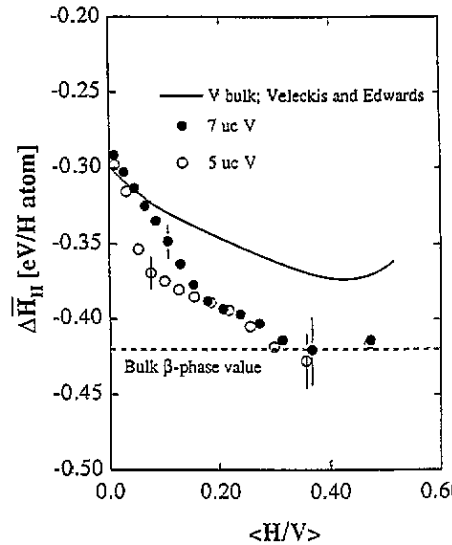

Figure 7. The heat of solution for the 5 u.c. and 7 u.c. Mo/V superlattices at different average hydrogen concentrations ⟨H/V⟩. The bulk values from Veleckis and Edwards [5] are also included.

The enthalpy change for the 5 and 7 u.c. samples are plotted against the hydrogen concentration $\langle H/V \rangle$ in figure 7, where the bulk vanadium enthalpy curve from Veleckis and Edwards is also shown for comparison [13]. The inserted error bars are the uncertainties from the fitting. The enthalpy change for the 5 u.c. and 7 u.c. samples reached a value of -0.42 eV per H atom after a steep increase from the infinite-dilution limit. This value of -0.42 eV per H atom is significantly larger than the bulk value, which is -0.37 eV per H atom. The heat of formation for the β-$VH_{0.5}$ hydride phase in bulk vanadium is also inserted in the figure (-0.42 eV per H atom) [14].

The enthalpy change at infinite dilution is approximately the same for both superlattices ($\Delta\bar{H}_H^{\infty} = -0.28$ eV per H atom) extrapolating the enthalpy curve to zero concentration of hydrogen. This is slightly lower than the value obtained for bulk vanadium ($\Delta\bar{H}_H^{\infty} = -0.30$ eV per H atom), but can be considered to be the same within the accuracy of the measurements. A significant shift is observed between the 7 u.c. enthalpy curve and the 5 u.c. curve for hydrogen concentrations up to 0.2. Above 0.2, the enthalpy curves are the same within the experimental uncertainties.

The entropy change is presented in figure 8 for the 5 u.c. and 7 u.c. superlattices together with bulk data. The solution entropies for the two superlattices are, within the experimental uncertainties, the same up to $\langle H/V \rangle = 0.05$. For hydrogen concentrations between 0.05 and 0.2, the entropy change for the 7 u.c. superlattice is slightly smaller than for the 5 u.c. superlattice, but they become equal at $H/V > 0.2$. The entropy change is larger in bulk vanadium than in the vanadium layers in the superlattice up to a hydrogen concentration of $\langle H/V \rangle = 0.2$. Above 0.2 the entropies are, within the experimental uncertainties, the same.

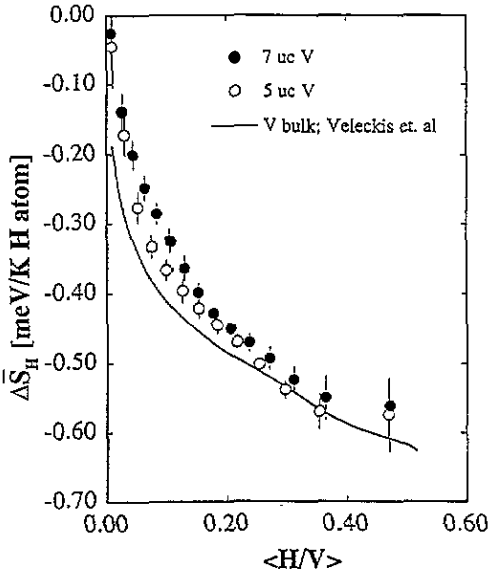

Figure 8. Entropy of solution for the Mo/V superlattices at different average hydrogen concentrations (H/V). The data obtained by Veleckis and Edwards [5] are also included.

5. Discussion

5.1. The enthalpy change

The enthalpy change for the 5 u.c. and 7 u.c. V lattices is significantly larger than the corresponding change in bulk vanadium. The hydrogen–hydrogen (H–H) interaction energy is therefore stronger in quasi-two-dimensional V lattices than in bulk V at low hydrogen concentrations and initially dependent on the layer thickness. In a Mo/V superlattice, the vanadium lattice is expanded in the substrate plane (the x–y direction) and contracted normal to the substrate plane (the z direction) [1]. The strain is therefore anisotropic in the V lattice. The enthalpy change should therefore be influenced by the anisotropic vanadium host lattice, since the H binding energy is highly sensitive to the strain state of the metal host. However, the enthalpy compared to bulk vanadium is the same for the 5 u.c. and 7 u.c. V lattices in the infinite-dilution limit, where a strain-induced change of the H-binding energy is most significant. The misfit strain alone can therefore not be the primary cause for the difference in $\Delta\bar{H}_H$ between the bulk vanadium and the two samples. The layer thicknesses and the clamping of the lattice with molybdenum must be considered in order to interpret the experimental data. The interaction between hydrogen atoms aligned in the z direction (see figure 1) is to a first approximation repulsive, since the energy required to expand the lattice is larger due to the epitaxy with the elastically harder Mo lattice. This effect is supposed to diminish with an increased layer thickness L_V. Hydrogen atoms can more easily reside in the plane of the vanadium lattice where the local volume is larger and the H–H interaction is supposed to be attractive. Within the elastic model for the H–H interaction proposed by Alefeld [4], this can be understood as a forced elastic dipole interaction in the x–y plane due to the asymmetric strain field in the V layers in the Mo/V superlattice. This is analogous to aligned electric dipoles in an external electric field. Increasing the layer thickness, the forced elastic dipole interaction become weaker

and eventually diminish at large layer thicknesses. The observed deviations in the enthalpy curves between 0.05 and 0.2 in hydrogen concentration for the 5 u.c. and 7 u.c. V samples are probably of this origin. Above 0.2, the forced interaction of hydrogen atoms in the plane become less pronounced and the enthalpy curve levels off.

5.2. The entropy change

The solution entropy of hydrogen in metals is given by the relation [15, 16]

$$\Delta \bar{S}_H - \tfrac{1}{2} S^0_{H_2} \tag{7}$$

where $\bar{S}_H$ is the entropy of the hydrogen atoms in the metal and $S^0_{H_2}$ is the standard entropy of the hydrogen gas at the chosen temperature. The entropy for the hydrogen atoms in the metal is divided into three different contributions as follows [15, 16]:

$$\bar{S}_H = \bar{S}_c + \bar{S}_v + \bar{S}_L \tag{8}$$

where $\bar{S}_c$ is the configurational term derived for one possible site for the hydrogen atom per metal atom and given by

$$\bar{S}_c = k_B \ln\left(\frac{c}{1-c}\right). \tag{9}$$

Here, c is the hydrogen concentration. The hydrogen atoms in the interstitial sites can be regarded as harmonic oscillators that all oscillate with the same frequency. The vibrational entropy can then be calculated with the Einstein expression [15, 16]

$$\bar{S}_v = 3k_B\{[x/\exp(x) - 1] - \ln[1 - \exp(-x)]\}. \tag{10}$$

Here, $x = h\nu/k_BT$ where ν is the frequency of oscillation and T the temperature. The last entropy term, $\bar{S}_L$, is due to the entropy arising from the lattice expansion derived in the thermodynamic analysis by Wagner [17] and can be given as

$$\bar{S}_L = \frac{\beta \bar{V}}{\kappa_T} \tag{11}$$

where β is the volume coefficient of thermal expansion, $\bar{V}$ is the partial molar volume of hydrogen in the metal and κ_T the coefficient of isothermal compressibility.

The configurational term, $\bar{S}_c$, describes the entropy when the hydrogen atoms are distributed in the lattice among the interstitial sites for hydrogen. Hydrogen occupies the tetrahedral position in the bcc lattice at the temperatures studied here [14]. Ideally, there are $n = 6$ tetrahedral sites per metal atom. Experimental entropy data from the bulk V–H system and other group-Vb metals are best represented by a configurational entropy expression with one hydrogen site per metal atoms [18, 19]. These experimental findings have been interpreted in terms of blocking of the six nearest-neighbour sites where the hydrogen atom resides. The best fit of (7) to the entropy data of Veleckis and Edwards give a number of hydrogen sites per metal atom of $n = 0.779$, compared to 1 for the ideal configuration entropy [13]. This non-ideal behaviour can be understood in terms of short-lived and correlated hydrogen configurations of atoms in the vanadium lattice, which effectively decreases the entropy. The entropy change is decreased for the quasi-two-dimensional

vanadium layers in the superlattices up to hydrogen concentrations of $\langle H/V \rangle = 0.2$ and reach the bulk data above 0.2. This implies a more disordered configuration for hydrogen up to 0.2 in hydrogen concentration, which can be interpreted as an extended α-phase.

The vibrational contribution to the entropy, $\bar{S}_\nu$, can be calculated knowing the vibrational energy for the hydrogen atom at the interstitial position. In bulk vanadium, the vibrational contribution can be calculated to be 0.06–0.08 meV K^{-1} per H atom using (10), and a vibrational energy for the hydrogen atom of roughly 165 meV [15]. The lattice parameter in the plane of the quasi-two-dimensional V layers are increased in the plane and slightly decreased normal to the plane [20], which is associated with an increased unit cell volume compared to bulk vanadium. The vibrational potential at the interstitial sites in the increased lattice-parameter part of the layer can be supposed to be broadened compared to bulk, due to the increased metal atom distance, and consequently the hydrogen atom vibrates with a lower frequency. The associated vibrational entropy can be estimated from figure 10 if the observed entropy change entirely originates from the vibrational contribution $\bar{S}_\nu$. The maximum shift in figure 8 between the bulk and superlattice entropy curves is roughly 0.1 meV K^{-1} per H atom at a hydrogen concentration of $\langle H/V \rangle = 0.1$. The vibrational entropy can therefore be determined to 0.16–0.18 meV K^{-1} per H atom in the superlattice. This corresponds to a vibrational energy of 100–120 meV for the hydrogen atom at the interstitial positions in the quasi-two-dimensional vanadium layers compared to the bulk value of 165 meV [15]. However, the concentration dependence of the superlattice entropy curves and the small decrease of entropy observed in the 5 u.c. compared to the 7 u.c. cannot be due to the change of the vibrational contribution alone.

The lattice expansion contribution, $\bar{S}_L$, for bulk vanadium has a value of roughly 0.07 meV K^{-1} per H atom in the temperature region 350–500 °C using values for the volume expansion coefficient, β, and the coefficient of isothermal compressibility, κ_T, for bulk vanadium [15]. The volume expansion coefficient, β, and the coefficient of isothermal compressibility, κ_T, for vanadium in a Mo/V superlattice are not known. The thermal volume expansion coefficient of vanadium can be assumed to be smaller in a superlattice than in bulk, due to the epitaxy with molybdenum and the limited size of the layers. Furthermore, the coefficient of isothermal compressibility κ_T is proportional to the elastic constants $(c_{11}+2c_{12})/3$ [21]. The elastic constants are not known for Mo/V superlattices, but are expected to increase in a superlattice structure. The partial molar volume of hydrogen $\bar{V}$ is considerably smaller for the superlattice than in bulk [22]. The lattice expansion entropy $\bar{S}_L$ is therefore expected to be smaller for the V layers than for bulk vanadium, in contrast with the experimental results.

6. Summary and conclusion

We have determined the hydrogen solubility and thermodynamics of quasi-two dimensional vanadium lattices of thicknesses 5 u.c. and 7 u.c. in Mo/V superlattices with resistometric methods. The hydrogen concentrations in the Mo/V superlattices were measured using the ^{15}H-method for hydrogen profiling to relate the excess resistivity to the hydrogen content. The maximum excess resistivity $\Delta\rho$ shifted to higher values at lower temperatures at a hydrogen concentration of H/V = 0.5. This is in contrast with previous published data, where $\Delta\rho$ remains constant for different temperatures and H/V = 0.5.

The enthalpy and entropy changes were deduced from the excess resistivity isotherms. The enthalpy change for vanadium in the superlattices reached a value of −0.42 eV per H atom after a steep increase from −0.28 eV per H atom at infinite dilution. The enthalpy

change for the 5 u.c. sample increased significantly faster than the 7 u.c. sample up to hydrogen concentrations of $\langle H/V \rangle = 0.2$. This can be understood as a forced in-plane elastic H–H interaction in the Mo/V superlattices due to the reduced dimensions and clamping invoked by the epitaxial relation to Mo. The entropy change $\Delta \bar{S}_H$ for the two superlattices is decreased compared to bulk data. This can be understood in terms of an extended α-phase in the quasi-two-dimensional V lattices and a broader vibrational potential for the hydrogen atom at the interstitial sites in the layers, but more detailed calculations of the entropy contributions must be performed in order to fully interpret the data.

Acknowledgments

The authors would like to acknowledge Åke Jönsson for his skilful work on the resistivity system and Jens Birch for most valuable help during the preparation of samples. Financial support from the Swedish National Research Council (NFR) is also greatly acknowledged.

References

[1] Hjörvarsson B, Rydén J, Karlsson E, Birch J and Sundgren J E 1991 *Phys. Rev.* B **43** 6440
[2] Hjörvarsson B, Ólafsson S, Stillesjö F, Karlsson E, Birch J and Sundgren J-E 1993 *Z. Phys. Chem.* Bd **181** 343
[3] Katsuta H and McLellan R B 1979 *J. Phys. Chem. Solids* **40** 845
[4] Alefeld G 1972 *Ber. Buns. Gesellschaft* **76** 746
[5] *Ólafsson S, Hjörvarsson B, Stillesjö F, Karsson E, Birch J and Sundgren J-E 1995 Phys. Rev. B accepted*
[6] Nordheim L 1931 *Ann. Phys.* **9** 607
[7] Kittel C *Introduction to Solid State Physics* 6th edn (New York: Wiley) ch. 21
[8] Pryde J A and Tsong I S T 1971 *Acta Metall.* **19** 1333
[9] Spulak R G Jr 1990 *J. Less. Common Met.* **160** 15
[10] Gurvitch M 1986 *Phys. Rev.* B **34** 540
[11] Birch J, Yamamoto Y, Hultman L, Radnoczi G, Sundgren J-E and Wallenberg L R 1990 *Vacuum* **41** 1231
[12] Lanford W A 1992 *Nucl. Instrum. Methods* B **66** 65
[13] Veleckis E and Edwards R K 1969 *J. Phys. Chem.* **73** 683
[14] Schober T and Wenzl H 1978 *Hydrogen in Metals: I. (Topics in Applied Physics 28)* (Berlin: Springer)
[15] Griffiths R, Pryde J A and Righini-Brand A 1972 *J. Chem. Soc. Faraday Trans. I* **68** 2344
[16] Kleppa O J, Dantzer P and Melnichak M E 1974 *J. Chem. Phys.* **61** 4048
[17] Wagner C 1971 *Acta Metall.* **19** 843
[18] Boreau G 1981 *J. Phys. Chem. Solids* **42** 743
[19] Oates W A, Lambert J A and Gallagher P T 1969 *Trans. Met. Soc. AIME* **245** 47
[20] Birch J 1994 *Thesis, Linköping University* ISBN 91-7871-452-4
[21] Peisl H 1978 *Hydrogen in Metals: I. (Topics in Applied Physics 28)* (Berlin: Springer)
[22] Stillesjö F, Hjörvarsson B and Zabel H 1994 *Phys. Rev.* B submitted